Synthesis of Low Cost Nanochitosan from Persian Gulf Shrimp Shell for Efficient Removal of Reactive Blue 29 (RB29) Dye from Aqueous Solution

Naghizadeh, Ali+*

Medical Toxicology and Drug Abuse Research Center (MTDRC), Birjand University of Medical Sciences, Birjand, I.R. IRAN

Ghofouri, Maryam

Department of Environmental Health Engineering, Student Research Committee, Faculty of Health, Birjand University of Medical Sciences, Birjand, I.R. IRAN

ABSTRACT: *Untreated wastewater disposal containing synthetic dyes produces serious problems in the environment. Industrial wastewater containing dye requires treatment by a suitable process before discharging into the environment. The present study has been performed as batch experimental study. Nanochitosan was synthesized from the Persian Gulf shrimp shell. The effect of the various parameters including pH, initial concentration of the RB29 dye, the equation contact time, and the adsorbent dosage as well as isotherm, thermodynamic and kinetic of the adsorption process were evaluated. The results of this study demonstrated that the maximum adsorption capacity of the nanochitosan, which occurred in pH=4, adsorbent dosage of 0.2 g/L, the concentration of 50 mg/L of RB29 dye and during 90 minutes, was 113.22 mg/g. Temkin and Dubinin-Radushkeish isotherms and pseudo second order kinetic equations have shown better results for describing the adsorption process. The entropic changes ($\Delta S°$) and enthalpy changes ($\Delta H°$) were 36.65J/mole K and 6.43 kJ/mole respectively. Also the Gibbs free energy (ΔG) was negative. Therefore nanochitosan can be used as a suitable low cost adsorbent for removal of RB29 dye from aqueous solutions.*

KEYWORDS: *RB29 dye; Nanochitosan; Adsorption; Isotherm; Thermodynamic; Kinetic.*

INTRODUCTION

The textile industry produces an important environmental problem due to consuming the huge amounts of water. Approximately, 200 to 350 m^3 water is consumed for producing one ton of textile production [1]. It is estimated that more than 10000 dyes are used in the textile industry. The concentrations of dyes in textile wastewater depending on type of coloring processes are in range of 100 to 100000 mg/L [2]. The global annual

** To whom correspondence should be addressed.*
+ E-mail: aliinaghizadeh@gmail.com
1021-9986/2019/6/93-103 11/\$/6.01

production of dye is more than 700000 tons, and approximately 2% of dyes are discharged into the wastewater [3]. Today, the synthetic dyes are used widely in the various industries including textile, leather, cosmetics, paper and paper-mill, inkjet printing, plastic, foods, medications, etc.[4] Regarding dyes are stable and resistant, and sometimes they are toxic, cancerous, and also mutagenic in human, discharging them into the environment leads to serious health, environmental, and aesthetic problems[5, 6]. Colors may interfere with antibacterial growth and prevent the photosynthesis of aquatic plants and also increase the Chemical Oxygen Demand (COD) of the water[7]. The presence of very small concentrations of dyes (less than 1 mg/L) in water is highly visible and is considered unpleasant[8]. Among the synthetic dyes, the azo dyes are used more than the others, and it is considered an important pollutant in the textile industries wastewater. Nearly, 50% of the global annual production of dye is the azo dyes [9]. The azo reactive dyes are specified by one or several nitrogen dual-band as azo bands. These dyes produce brighter dyeing, and also they have suitable dyeing rate, simple technique, and lower energy consumption. These dyes are water soluble and in the form of hydrolyzed. Therefore, they cannot be removed easily from the wastewater by common treatment processes [10]. Various methods including adsorption, coagulation, biodegradation and chemical synthesis have been used for treatment and decolonization of the colored wastewater [11]. It has been reported that the reactive dyes have been adsorbed on the weak biomasses that have not degraded under the aerobic condition [12]. Coagulation process produces a lot of sludge and the cost of its sludge disposal is high. The process of the ion exchange is not adopted for wide range of the dyes and it has high cost. The membrane separation process affects the dye adsorption. However, some problems such as its relatively high investment and membrane fouling are its limitations for dye removal. The adsorption process is more suitable than the other methods, because it has lower cost, simpler design, efficiency, availability, effectiveness and lack of sensitivity to the toxic material [13]. Recently, it has been attempted that the cost-effective materials are used as adsorbent in the tertiary treatment of wastewater [14]. In the nature, chitin is the second most abundant polysaccharide after cellulose [15]. The recent progresses in the field of nanotechnology have provided the opportunities for developing the water supply systems for next generations. In the recent years, the highly efficient, modular, and multidisciplinary processes are provided by nanotechnology. By less rely on large infrastructure, it is expected that the nanotechnology provides efficient solution for treatment of water and wastewater. Nanotechnology not only has overcome the major challenges in the available treatment technology, but also it provides a new capacity for treatment the unusual water resource and its economic usage [16]. Compare to auxiliary micro-sized devices which are used in the separation process, the nano-sized adsorbents have suitable function due to the high surface area, small size, and the quantum size [17]. Nanochitosan prepared by using the usual coagulation reaction between amine groups with the positive charge of chitosan to ions of sodium tripolyphosphate with negative charge [18]. The size and the dosage are important parameters for adsorption of the pollutants onto nanochitosan as an adsorbent. These factors determine the adsorbent capacity for given initial concentration of adsorbent. Nanochitosan has high load density than the other coagulants. The density of the load of this polymer increases by its higher adsorption which confirms the rapidly destabilization of the particles. Also, nanochitosan can be used as environmental compatible material for wastewater treatment [19]. The main methods for preparing the nanochitosan include: linked emulsion, mixture of emulsion/ drop, gelatin/ion therapy, sequestration/ density, reverse micelle, template polymerization, and self-made molecular method [20]. *Guo et al.* removed the dye by using the bentonite-modified Chitosan [21]. *Travlou et al.* removed the reactive dyes by using the Chitosan composite/ graphene oxide [22]. Also, *W Ngah et al*. [23] and *Mahmoodi et al.* [24] removed the dye by using the modified chitosan. The characteristics of the reactive blue 29 dye have been shown in the Table 1.

In this study, the removal of RB29 dye was investigated using Nanochitosan as an adsorbent.

EXPERIMENTAL SECTION

This is an experimental practical study that has been performed as batch condition. In this study, the function of nanochitosan as an adsorbent for removing the RB29 dye from the aqueous solution in the lab scale has been studied.

Table 1: The characteristics of the RB29 dye [25].

Chemical structure	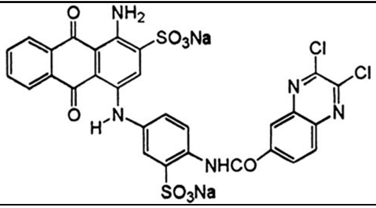
Symbol	RB29
Chemical formula	$C_{29}H_{15}C_{12}N_5Na_2O_9S_2$
The Wavelength of maximum adsorption λmax (nm)	589
Molecular weight g/mole	788

The commercial RB29 dye with molecular weight 788 g/mole was purchased from the Sigma Aldrich Company and it has been used without further purification. Also, sodium tripolyphosphate with molecular weight of 367.86 mg/mole and purity 57-59% was purchased from Scarlau Company. In addition, in this study the required chemical materials including acetic acid, NaOH, and HCl were bought from the Merck Company. The images of the Scanning Electron Micrographs (SEM) with high magnification and resolution were prepared for investigating and observing the samples, and also X-ray Diffraction (XRD) spectroscopy with X' Pert Pro system was prepared from Panalytical Company for analyzing the structural properties of adsorbent such as size and shape of the nanochitosan.

Synthesis and preparation of the adsorbent

The shell of the shrimp as fishery waste of the caught shrimp was prepared by the Persian Gulf Fishery. Chitin has been prepared during two main steps including 1) demineralization: completely removing minerals with diluted mineral acid, 2) deproteinization: to remove the organic materials [26]. Demineralization has been doneduring 15 min at the room temperature in the presence of HCl 0.25 molar (the ratio of solid to liquid 1/40 (w/v)), and also deproteinization has been performed with 1 molar NaOH at the temperature of 70° C during 24 hours[27]. In the next stage, Chitosan was extracted from chitin by NaOH 70% [28]. According to the Tang et al studies [17], nanochitosan was synthesized as follow: 20 mg of Chitosan solved in 40 mL acetic acid 2.5% (v/v), then 20 mL of sodium tripolyphosphate with concentration of 0.75 mg/mL was added gradually to the shaking acetic acid solution. The rate of shaker was set at 240 rpm for preparing the nanochitosan. Nanochitosan were produced as milky suspension. After that the top layer of the suspension was discarded, then the solution was centrifuged at 5000 rpm. At all the stages, the jelly material was dried in the desiccator at the room temperature. Then it was Powdered.

Adsorption experiments

After preparing the RB29 dye stock solution, the solutions with primary concentration of 10, 20, 30, and 50 mg/L have been made by diluting the solution. The effect of various parameters including pH, the initial concentration of the dye, adsorbent dose, the contact time, and the effect of temperature on the adsorption process were investigated. Also, isotherms, thermodynamic, and kinetic process were evaluated. The range of each variable parameter including various initial concentration of RB29 dye (10-50 mg/L), pH (3-9), and different doses of nanochitosan (0.2-0.75 g/L) had been studied at different contact times (2-90 minutes). At the all steps of the experiment, the effect of each parameter was investigated by the variation of the considered parameter and the other invariables. Then the isotherm models of Langmuir, Freundlich, Temkin, and Dubinin- Radushkevich were determined. The optimized concentration of dye and the optimized adsorbent dosage were selected, and the pH of the solutions was set on the optimized pH for evaluating the effect of the temperature on the efficacy of the adsorption process. The RB29 solutions were stirred at the 15, 30, 40, and 50° C during 90 minutes at incubator's shaker. At the end, the Erlenmeyer flasks were removed and the samples were centrifuged and filtered by two filters with pore size of 0.2 µm. The final concentration of the RB29 dye was determined by +UV/VIS Spectrometer T80 at wavelength of 589 nm. The adsorption capacity of nanochitosan was calculated by the nanochitosan with the following equation:

$$q_e = \frac{(C_o - C_e)\times V}{M} \quad (1)$$

Where:

qe: equilibrium amount of adsorbent (mg /g)

C_0: initial concentration of the RB29 (mg/L)

C_e: final concentration of the RB29 (mg/L)

M: mass of the adsorbent (g)

V: volume of the solution (L)

Equations (2) and (3) were used for determination the adsorption thermodynamics:

$$\Delta G = -RTLnK_c \quad (2)$$

Where:

$\Delta G°$: the Gibbs free energy changes (kJ/mole)

R: universal gas constant equal to 8.314 J/mole K

T: temperature (K)

K_c: thermodynamic equilibrium constant

$$LnK_c = \frac{\Delta S^\circ}{R} - \frac{\Delta H^\circ}{RT} \quad (3)$$

Where:

$\Delta S°$: standard entropy changes

$\Delta H°$: standard enthalpy changes

After calculating the thermodynamic equilibrium constant for different temperatures and related free energy, the diagram ln K_c against 1/T was plotted. The slope and intercept of the chart were used for determination of ΔS and ΔH, respectively.

Also in this study Freundlich and other isotherms including Langmuir were used for describe the adsorption behavior of dye molecules onto adsorbent materials. Equations (4) and (5) are linearized form of Langmuir and Freundlich isotherms respectively:

$$\frac{c_e}{q_e} = \frac{1}{q_{max}\times k_1} + \frac{C_e}{q_{max}} \quad (4)$$

$$Lnq_e = \left(\frac{1}{n}\right)LnC_e + Lnk_f \quad (5)$$

Where:

q_e: equilibrium concentration of dye in the solid phase (mg/g)

q_{max}: maximum adsorption capacity (mg/g)

k_l: adsorption equilibrium constant (L/mg)

k_f: Freundlich constant ($mg^{1-1.n}$ $L^{l/n}$ /g) which demonstrates the adsorption capacity, and

n: constant which shows the severity of the adsorption.

For investigating the equilibrium data, two common models of kinetic (pseudo first order and pseudo second order) were used for studying the kinetic of adsorption. The correlation coefficient (R^2) has been considered as a criterion for agreement between the experimental data and two suggested models.

The pseudo first order kinetic or equation (Lagergren 1898) is as follow:

$$Log(q_e - q_t) = \log q_e - \frac{k_1}{2.303}t \quad (6)$$

Where:

q_e: the rate of the adsorbed material on the adsorbent in the time t according to mg/g.

q_t: the rate of the adsorbed material on the adsorbent in the equilibrium time according to mg/g.

k_1: the adsorption rate constant pseudo first order kinetic (L/min)

The chart of Log (q_e – q_t) against t is used for determining the k constant and q_e.

The pseudo second order kinetic (Ho and Mckay 2000) is as follow:

$$\frac{t}{qt} = \frac{1}{k_2 q_e^2} + \frac{t}{q_e} \quad (7)$$

k_2: is the constant adsorption of the pseudo second order kinetic (g/ (mg/min)). The diagram of t/q_t against t has been used for obtaining the rate parameters. The amounts of q_e and k_2 were determined by calculating the slope and the intercept of this diagram.

RESULTS AND DISCUSSION

Specification and characterization of the synthesized nanochitosan

Scanning electron microscope (SEM) is a main and powerful magnification tool for study of the morphological structure of adsorbents. Fig. 1 shows the SEM image of nanochitosan. Regarding to this figure, nanochitosan have sheet structure.

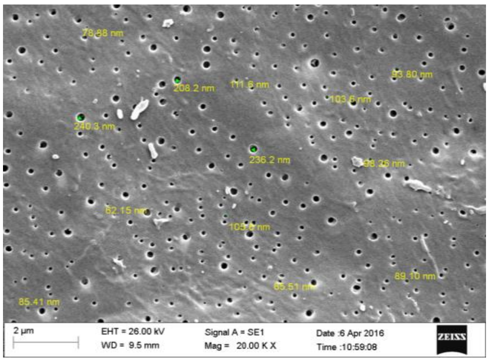

Fig. 1: Scanning electron microscope (SEM) image of nanochitosan.

Fig. 2 demonstrates the XRD of nanochitosan by X' pert Pro system which was prepared by Panalytical Company. XRD of chitosan indicates the two obvious peaks in 2θ= 10˚ and 2θ=20˚ which has been shown in the Fig. 2(a). XRD of nanochitosan indicates two wide peaks in the 2θ=11˚ and 2θ=20-25˚ which states the changes in the peaks of chitosan to wider peaks in the nanochitosan. Also, it shows increased non-crystallized form and decreased crystallized structure of chitosan after cross-linking to sodium tripolyphosphate. Crystallization of chitosan is a key parameter for accessing its internal sites[17].

Effects of pH

In this study, the effect of pH of the solution with the range of 3 to 9 on the rate adsorption of the RB29 dye was evaluated by nanochitosan. Fig. 3 shows the results of the effect of pH on the adsorption of RB29 dye by nanochitosan.

According to Fig. 3, adsorption of the RB29 dye onto nanochitosan at the concentration of 10 mg/L and pH=4 is 47.16 mg/g. The results of this Figure shows that nanochitosan in pH=4 has the most adsorption capacity, and the adsorption capacity has decreased at higher pHs. *Chiou et al.* (2003) concluded that the capacity of the dye adsorption onto chitosan decreases at higher pHs. In the lower pH, however more protons are available for protonation of the amine groups of the nanochitosan molecules in the form of $–NH3^+$. As a result, the electrostatic attraction between molecules of dye and adsorption sites is increased and it results in dye adsorption [29]. The results of the *Zhu et al.* [30] and also *Sun et al*. [31] and *Naddafi et al.* [32] are agreement to the result of the present study.

Effect of contact times and initial concentrations

Fig. 4 indicates the results of initial concentrations and contact times for adsorption of RB29 dye on to nanochitosan.

According to Fig. 4, the adsorption capacity in the all concentrations would be balanced after 90 minutes. After 90 minutes, the rates of adsorption for adsorbent mass in the concentrations of 10, 20, 30, and 50 mg/L are 25.02, 49.98, 70.38, and 113.32 mg/g, respectively. With regard to the obtained results from the diagram, the adsorption capacity has been increased by increased contact time; however, it has been balanced in the all concentrations in 90 minutes. *Dawood et al.* (2002) in their study concluded that the adsorption capacity in the all concentrations increased at higher contact times, and the equilibrium was achieved after 100 minutes. For this reason, the primary dye provides kinetic force between solid and liquid phases for overcoming the mass transfer. Also, in the primary period of the exposure the dye adsorption is very fast on the powered pine cones by using adsorption; however, it become slower over the time[33].

Effect of adsorbent mass

The results of adsorbent dose (0.2-0.75 g/L) on adsorption of RB29 dye onto nanochitosan have been indicated in the Fig. 5.

With regard to the results of this experiment and the diagram of the adsorption capacity for the mass of adsorbent, it is observed that the adsorption capacity is decreased by higher dose of adsorbent. The most adsorption capacity was in the adsorbent dose of 0.2 g/L. therefore, this adsorbent dose was selected as optimized dose in the experiments. The results demonstrated that the adsorption capacity of nanochitosan is decreased by increasing mass of adsorbent. Sulak et al in their study (2007) obtained the similar results [34]. There is two reasons for this phenomenon: 1) increased mass of adsorbent in the stable concentration and volume of dye causes unsaturated adsorption sites, and 2) decreased capacity of adsorbent may be due to particle aggregation result from higher mass of adsorbent[35].

Adsorption isotherms

The results of the calculations for isotherms factors of Freundlich, Langmuir, Temkin and Dubinin-Radushkevich has been shown in the Table 2. With

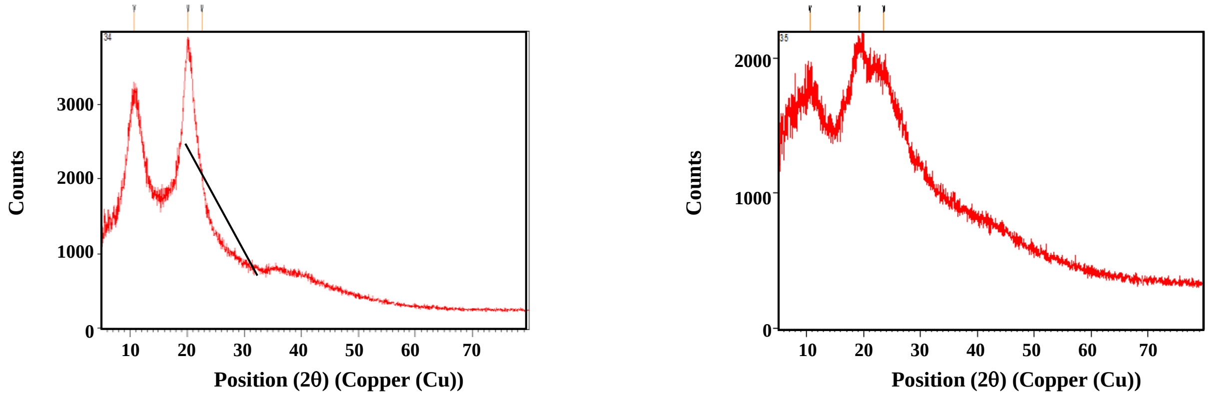

Fig. 2: X-ray diffraction (XRD) of (a) chitosan and (b) nanochitosan.

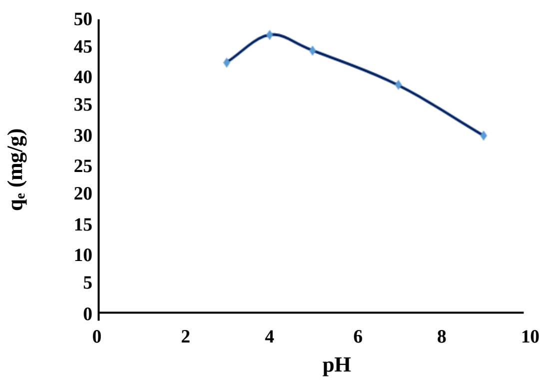

Fig. 3: The effect of the pH of the solution on the RB29 dye adsorption by nanochitosan.

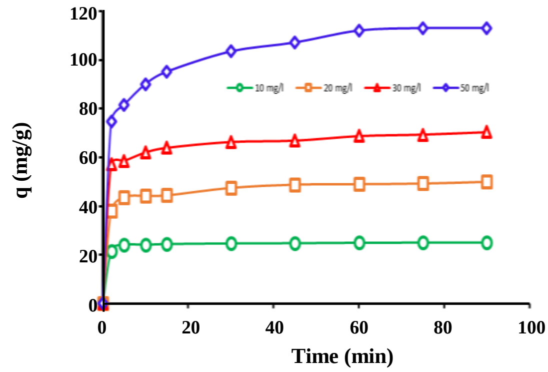

Fig. 4: The Effect of contact times and initial concentrations on adsorption of RB29 by nanochitosan.

regard to the comparison between R^2 factors as well as other parameters, the adsorption of RB29 dye by nanochitosan follows isotherm of Temkin and then Dubinin- Radushkevich.

Adsorption isotherms show that how an adsorbed molecule distributes between solid and liquid phases when the adsorption process reaches equilibrium. Analyzing the isotherm data by matching them to the various isotherm models is an important step for designing a model which can be used for this purpose. Also, it is vital for optimizing the adsorbent usage [36]. Isotherm of Langmuir explains one layer of absorbable article on the external layer of adsorbent; however, isotherm of Freundlich is used for describing the adsorbent features on the heterogeneous surface [37]. Temkin isotherm includes one factor which contains adsorbent- adsorbate interactions by ignoring the much higher and much lower rate of concentrations. This model proposed that the heat adsorption of all molecules has linear reduction instead of logarithmic procedure [38]. Isotherm of Dubinin- Radushkevich have been used for adsorption mechanism with Gaussian energy distribution on the heterogeneous surface[39]. With regard to the factors of the calculated isothermal models for adsorption process, the Temkin and Dubinin- Radushkevich isotherm models are more suitable than the other models for adsorption data at the studied concentration range with the amount of R^2= 0.99. Elkady et al study also indicated that isothermal data is coincident to the results of the Temkin model, and this is agreement to the result of the present study[40].

Effect of temperature and thermodynamic on the process

Fig. 6 has been demonstrated the results of evaluating the solution temperature and thermodynamic parameters

Table 2: The factors of the isotherm models for RB29 dye adsorption by nanochitosan.

Isotherms	Constants	Values
Langmuir	q_{max} (mg/g)	985.17
	K_L (L/mg)	0.015
	R_L	0.50
	R^2	0.9
Freundlich	k_f (mg/g)	19.43
	1/n	0.91
	n	1.09
	R^2	0.91
Temkin	A_T, L/mg	0.52
	b_T (J/mole)	25.28
	B	98
	R^2	0.99
Dubinin-Radushkevich	β, mole^2/kJ^2	3.357E-06
	E, kJ/mole	0.3859
	q_m, mg/g	200.3024
	R^2	0.99

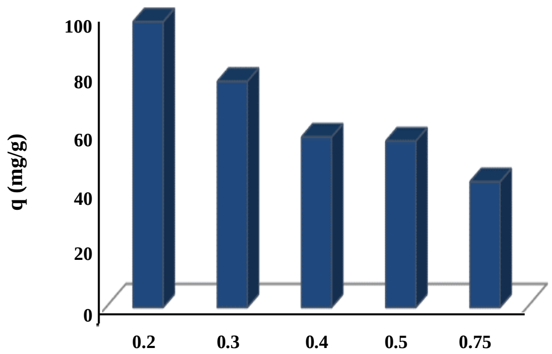

Fig. 5: The effect of adsorbent dose on the rate of RB29 dye adsorption by Nanochitosan.

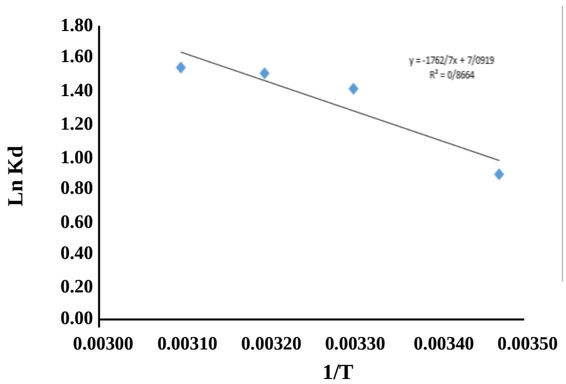

Fig. 6: The linear plot of In Kd against l/T for adsorption of RB29 dye by nanochitosan.

on the efficacy of the adsorption process of RB29 dye onto nanochitosan. With regard to the calculated parameters in the Table 3, the negative amounts of ΔG ° and the positive amounts of ΔS ° shows the spontaneous and endothermic adsorption reaction of the RB29 dye by nanochitosan. It is observed that increased temperature of the solution resulted in higher adsorption capacity of the dye.

After calculating either the thermodynamic equilibrium constant for different temperatures or related free energy, the diagram of In K_d was drawn against l/T. The negative rate of ΔG states the spontaneous process of adsorption in the nature. However, the positive rate of ΔH° equal to 6.43 kJ/mole shows that the adsorption process is naturally endothermic[38]. The positive rate of standard entropy changes of

Table 3: Calculated thermodynamic parameters of RB29 dye adsorption onto nanochitosan.

Adsorbent	T (K)	qe (mg/g)	Thermodynamics Parameters		
			ΔG (kJ/mole)	ΔH (kJ/mol)	ΔS (J/mol K)
Nanochitosan	288	138.465	-4.18	6.43	36.65
	303	142.22	-4.54		
	313	152.955	-5.13		
	323	157.785	-5.51		

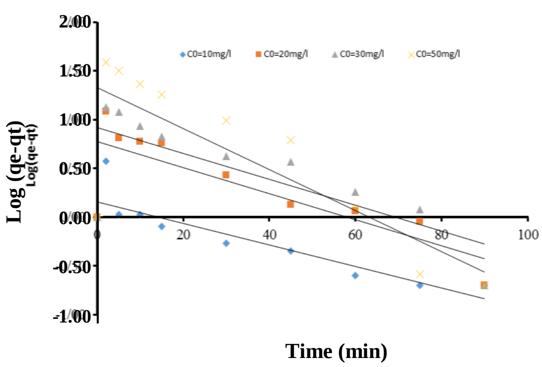

Fig. 7: Pseudo first order kinetic model for adsorption of the RB29 dye by nanochitosan.

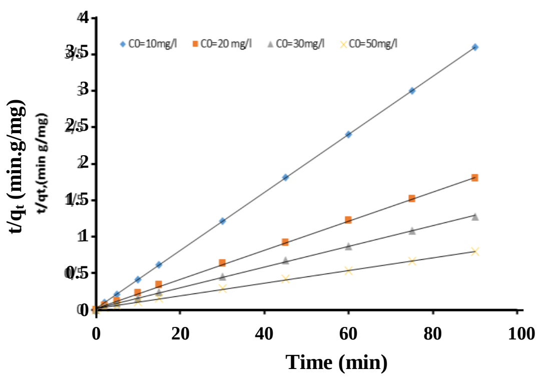

Fig. 8: Pseudo second order kinetic model for adsorption of the RB29 dye by nanochitosan.

ΔS° equal to 36.65 J/mole K states that the freedom degree between solid and liquid phases has been increased during the adsorption[41] The result of the Tan et al research is in accordance with the result of the present study[17].

Adsorption kinetics

Regarding to Figs. 7 and 8 as well as Table 4 it is observed that with regard to the amount of the R^2 factors in both two kinetics models the adsorption process is described better by pseudo second order kinetic model.

In the pseudo second order kinetic model, the adsorption capacity which has been calculated by the kinetic equations (q_e,cal) is closer to the absorption capacity which has been obtained in the adsorption experiments ($q_{e,}$exp). Also, the amount of the R^2 factor in the pseudo second order kinetic model is higher than pseudo first order kinetic model. Therefore, this shows that adsorption process is coincident to the pseudo second order kinetic model. The result of the previous study [42-43] are in agreement with the result of the present study.

CONCLUSIONS

In this study, nanochitosan has been synthesized from the shell of the shrimp during three stages, and also it has been used for removing the RB29 dye from water solution. The maximum adsorption capacity of the nanochitosan, in RB29 dye concentration of 50 mg/L was 113.22 mg/g. Temkin and Dubinin-Radushkeish isotherms and pseudo second order kinetic equations have shown better results for describing the adsorption process. The adsorption process was naturally endothermic. The positive rate of ΔS° was stated that the freedom degree between solid and liquid phases has been increased during the adsorption. With regard to the results, it can be suggested that nanochitosan is a suitable low cost nanomaterial for removing the RB29 dye from aqueous solution.

Acknowledgement

The authors are grateful to the deputy of research of Birjand University of Medical Sciences for the financial support (code: 455256) as well as all the laboratory staffs of department of environmental health engineering and also the Medical Toxicology and Drug Abuse Research Center.

Table 4: The factors of the calculated kinetics models for adsorption of the RB29 dye by nanochitosan.

Adsorbent	C_0 (mg/L)	Pseudo-first-order			Pseudo-second-order			q_e,exp (mg/g)
		K_1 (min^{-1})	q_e, cal (mg/g)	R^2	K_2 (g/mg min)	q_e,cal (mg/g)	R^2	
nanochitosan	10	0.03	1.44	0.81	0.13	25.08	1.00	25.22
	20	0.03	5.94	0.66	0.02	50.09	1.00	50.18
	30	0.03	8.29	0.57	0.01	70.35	1.00	70.58
	50	0.05	21.42	0.64	0.00	115.14	1.00	113.42

Received : Jun. 5, 2018 ; Accepted : Oct. 8, 2018

REFERENCES

[1] Gozálvez-Zafrilla J., Sanz-Escribano D., Lora-García J., Hidalgo M.L., Nanofiltration of Secondary Effluent for Wastewater Reuse in the Textile Industry, *Desalination*, **222**(1-3): 272-279 (2008).

[2] Figueroa S., Vazquez L., Alvarez-Gallegos A., Decolorizing Textile Wastewater with Fenton's Reagent Electrogenerated with a Solar Photovoltaic Cell, *Water Research*, **43**(2): 283-294 (2009).

[3] Ip A.W., Barford J.P., McKay G., A Comparative Study on the Kinetics and Mechanisms of Removal of Reactive Black 5 by Adsorption onto Aactivated Carbons and Bone Char, *Chemical Engineering Journal*, **157**(2-3): 434-442 (2010).

[4] Zhang L., Cheng Z., Guo X., Jiang X., Liu R., Process Optimization, Kinetics and Equilibrium of Orange G and Acid Orange 7 Adsorptions onto Chitosan/Surfactant, *Journal of Molecular Liquids*, **197**: 353-367 (2014).

[5] Elkady M., Ibrahim A.M., El-Latif M.A., Assessment of the Adsorption Kinetics, Equilibrium and Thermodynamic for the Potential Removal of Reactive Red Dye Using Eggshell Biocomposite Beads, *Desalination*, **278**(1-3): 412-423 (2011).

[6] Carneiro P.A., Umbuzeiro G.A., Oliveira D.P., Zanoni M.V.B., Assessment of Water Contamination Caused by a Mutagenic Textile Effluent/Dyehouse Effluent Bearing Disperse Dyes, *Journal of Hazardous Materials*,**174**(1-3): 694-699 (2010).

[7] Shojaei S., Shojaei S., Experimental Design and Modeling of Removal of Acid Green 25 dye by Nanoscale Zero-Valent Iron, *Euro-Mediterranean Journal for Environmental Integration*, **15**(2): 1-7 (2017).

[8] Hajiaghababaei L., Abozari S., Badiei A., Zarabadi Poor P., DehghanAbkenar S., Ganjali M.R., et al. Amino Ethyl-Functionalized SBA-15: A Promising Adsorbent for Anionic and Cationic Dyes Removal, *Iranian Journal of Chemistry and Chemical Engineering (IJCCE)*, **36**(1): 97-108 (2017).

[9] Maljaei A., Arami M., Mahmoodi N.M., Decolorization and Aromatic Ring Degradation of Colored Textile Wastewater Using Indirect Electrochemical Oxidation Method, *Desalination*, **249**(3): 1074-8 (2009).

[10] Tunc Ö., Tanacı H., Aksu Z., Potential Use of Cotton Plant Wastes for the Removal of Remazol Black B Reactive Dye, *Journal of Hazardous Materials*, **163**(1):187-98 (2009).

[11] Yu S., Liu M., Ma M., Qi M., Lü Z, Gao C., Impacts of Membrane Properties on Reactive dye Removal from Dye/Salt Mixtures by Asymmetric Cellulose Acetate and Composite Polyamide Nanofiltration Membranes, *Journal of Membrane Science*, **350**(1-2): 83-91 (2010).

[12] Andrade L.S., Ruotolo L.A., Rocha-Filho R.C., Bocchi N., Biaggio S.R., Iniesta J., García-Garcia V., Montiel V., On the Performance of Fe and Fe, F doped Ti–Pt/PbO2 Electrodes in the Electrooxidation of the Blue Reactive 19 Dye in Simulated Textile Wastewater, *Chemosphere*, **66**(11): 2035-43 (2007).

[13] Sharma P., Kaur H., Sharma M., Sahore V., A Review on Applicability of Naturally Available Adsorbents for the Removal of Hazardous Dyes from Aqueous Waste, *Environmental Monitoring and Assessment*, **183**(1-4):151-95 (2011).

[14] Kyzas G.Z., Fu J., Matis K.A., The Change from Past to Future for Adsorbent Materials in Treatment of Dyeing Wastewaters, *Materials*, **6**(11):5131-58 (2013).

[15] Lee C.G., Chitin, Chitinases and Chitinase-Like Proteins in Allergic Inflammation and Tissue Remodeling, *Yonsei Medical Journal*, **50**(1):22-30 (2009).

[16] Qu X., Alvarez P.J., Li Q., Applications of Nanotechnology in Water and Wastewater Treatment, *Water Research*, **47**(12): 3931-3946 (2013).

[17] Sivakami M., Gomathi T., Venkatesan J., Jeong H-S., Kim S-K., Sudha P., Preparation and Characterization of Nano Chitosan for Treatment Wastewaters, International Journal of Biological Macromolecules, **57**: 204-212 (2013).

[18] Hu Z., Zhang J., Chan W., Szeto Y., The Sorption of Acid Dye onto Chitosan Nanoparticles, *Polymer*, **47**(16):5838- 5842 (2006).

[19] Kana M., Radi M., Elsabee M.Z., Wastewater Treatment with Chitosan Nano-Particles, *International Journal of Nanotechnology and Application*, **3**(2): 39-50 (2013).

[20] Perera U., Rajapakse N., Chitosan Nanoparticles: Preparation, Characterization, and Applications. Seafood Processing by-Products, *Springer*, 371-87 (2014).

[21] Guo J, Chen S, Liu L, Li B, Yang P, Zhang L, Feng Y.Adsorption of Dye from Wastewater Using Chitosan–CTAB Modified Bentonites, *Journal of Colloid and Interface Science*, **382**(1): 61-66 (2012).

[22] Travlou N.A., Kyzas G.Z., Lazaridis N.K., Deliyanni E.A., Graphite Oxide/Chitosan Composite for Reactive Dye Removal, *Chemical Engineering Journal*, **217**: 256-265 (2013).

[23] Wan Ngah W.S., Ariff N.F.M., Hashim A., Hanafiah M.A.K.M., Malachite Green Adsorption onto Chitosan Coated Bentonite Beads: Isotherms, Kinetics and Mechanism, *CLEAN–Soil, Air, Water*, **38**(4):394-400 (2010).

[24] Mahmoodi N.M., Salehi R., Arami M., Bahrami H., Dye Removal from Colored Textile Wastewater Using Chitosan in Binary Systems, *Desalination*, **267**(1):64-72 (2011).

[25] Machado FM, Bergmann CP, Lima EC, Adebayo MA, Fagan SB. Adsorption of a textile dye from aqueous solutions by carbon nanotubes, *Materials Research*, **17**:153-60 (2014).

[26] Rhazi M., Desbrieres J., Tolaimate A., Alagui A, Vottero P., Investigation of Different Natural Sources of Chitin: Influence of the Source and Deacetylation Process on the Physicochemical Characteristics of Chitosan, *Polymer International*, **49**(4): 337-344 (2000).

[27] Percot A., Viton C., Domard A., Optimization of Chitin Extraction From Shrimp Shells, *Biomacromolecules*, **4**(1):12-18 (2003).

[28] Islam M.M., Masum S.M., Rahman M.M., Molla M.A.I., Shaikh A., Roy S., Preparation of Chitosan From Shrimp Shell and Investigation of Its Properties, *Int J Basic Appl Sci.*, **11**(1):116 - (2011).

[29] Chiou M., Li H., Adsorption Behavior of Reactive Dye in Aqueous Solution on Chemical Cross-Linked Chitosan Beads, *Chemosphere*, **50**(8):1095-1105 (2003).

[30] Zhu H-Y., Jiang R., Xiao L., Li W., A Novel Magnetically Separable γ-Fe_2O_3/Crosslinked Chitosan Adsorbent: Preparation, Characterization and Adsorption Application for Removal of Hazardous Azo Dye, *Journal of Hazardous Materials*, **179**(1-3): 251-257 (2010).

[31] Sun XF, Wang SG, Cheng W, Fan M, Tian BH, Gao BY, Li XM. Enhancement of Acidic Dye Biosorption Capacity on Poly (ethylenimine) Grafted Anaerobic Granular Sludge, *Journal of Hazardous Materials*, **189**(1-2): 27-33 (2011).

[32] Naddafi K, Nabizadeh Nodehi R. Removal of reactive blue 29 dye from water by single-wall carbon nanotubes, *Iranian journal of health and environment*, **3**(4):359-68(2011).

[33] Dawood S., Sen T.K., Removal of Anionic Dye Congo Red from Aqueous Solution by Raw Pine and Acid-Treated Pine Cone Powder as Adsorbent: Equilibrium, Thermodynamic, Kinetics, Mechanism and Process Design, *Water Research*, **46**(6): 1933-1946 (2012).

[34] Sulak M., Demirbas E., Kobya M., Removal of Astrazon Yellow 7GL from Aqueous Solutions by Adsorption onto Wheat Bran, *Bioresource Technology*, **98**(13): 2590-2598 (2007).

[35] Cardoso N.F., Pinto R.B., Lima E.C., Calvete T., Amavisca C.V., Royer B., et al. Removal of Remazol Black B Textile Dye from Aqueous Solution by Adsorption, *Desalination*, **269**(1-3):92-103 (2011).

[36] Shirzad-Siboni M., Fallah S., Tajasosi S., Removal of Acid Red 18 and Reactive Black 5 Dyes from Aquatic Solution by Using of Adsorption on Azollafiliculoides: a Kinetic Study, *Journal of Guilan University of Medical Sciences*, **22**(88): 42-50 (2014).

[37] Ashtekar V., Bhandari V., Shirsath S, Jolhe Pscp, Ghodke S., Dye Wastewater Treatment: Removal of Reactive Dyes Using Inorganic and Organic Coagulants, *I Control Pollution*, **30**(1): 33 (2013).

[38] Dareini F., Amini M.A., Zarei S.H., Saghi M.H., Removal of Acid Black 1 Dye from Aqueous Solution Using Nano-Iron Particles, *Journal Of Sabzevar University Of Medical Sciences* ,**20**(5); 782-790 (2014).

[39] Ehrampoush M., Ghanizadeh G., Ghaneian M., Equilibrium and Kinetics Study of Reactive Red 123 Dye Removal from Aqueous Solution by Adsorption on Eggshell, *Journal of Environmental Health Science & Engineering.* **8**(2):101-6 (2011).

[40] Thinakaran N., Baskaralingam P., Pulikesi M., Panneerselvam P., Sivanesan S., Removal of Acid Violet 17 from Aqueous Solutions by Adsorption Onto Activated Carbon Prepared From Sunflower Seed Hull, *Journal of Hazardous Materials*, **151**(2-3): 316-322 (2008).

[41] Hyung H, Kim JH. Natural Organic Matter (NOM) Adsorption to Multi-Walled Carbon Nanotubes: Effect of NOM Characteristics and Water Quality Parameters. *Environmental Science & Technology*, **42**(12):4416-21 (2008).

[42] Chinoune K, Bentaleb K, Bouberka Z, Nadim A, Maschke U. Adsorption of Reactive Dyes from Aqueous Solution by Dirty Bentonite, *Applied Clay Science*., **123**:64-75 (2016).

[43] Najafi Saleh A., Dehghani M.H., Nabizadeh R., Mahvi A.H., Yaghmaeian K., Faraji H., Ghaderpoori M., Yousefi M., Mohammadi A.A., Data on the Acid Black 1 Dye Adsorbtion from Aqueous Solutions by Low-Cost Adsorbent- Cerastoderma Lamarcki Shell Collected From the Northern Coast of Caspian Sea, *Data in Brief*, **17**: 774-780 (2018).